Visible-light-driven Photodegradation of Commercial Dyes by the Cooperation of Co-doped TiO_2 Material

Russameeruk Noonuruk and Chakkaphan Wattanawikkam*

Division of Physics, Faculty of Science and Technology, Rajamagala University of Technology Thanyaburi, Pathum Thani, Thailand

Received: 14 March 2019, Revised: 16 August 2019, Accepted: 10 October 2019

Abstract

The Co-doped TiO_2 photocatalysts with various contents of Co were fabricated by co-precipitation method combined with calcinations at 500°C. Two different dyes of rhodamine b and methylene blue were used to evaluate the photocatalytic performance of the prepared samples. The different concentration of Co has significant influence on structural, morphological, optical properties as well as photocatalytic activity of TiO_2 catalyst. The XRD diffraction patterns of all samples exhibit the anatase phase. X-ray photoelectron spectroscopy technique was used to investigate the chemical state of prepared samples. The BET measurement shows larger specific surface area of doped samples than that of pure TiO_2. The incorporation of Co ions into TiO_2 results in the red-shift in photo-absorption of samples toward visible region. The photocatalytic activities on rhodamine b and methylene blue dyes degradation clearly show that the performance of photodegradation highly depends on the concentration of dopant contents and type of organic dyes. The Co-doped TiO_2 sample with 3% of Co dopant concentration exhibited superior photodegradation rate under visible light illumination in both of rhodamine b and methylene blue dyes. The influences of dopant ions and concentration on physical properties, optical absorption and photocatalytic activity on TiO_2 are also discussed.

Keywords: Co-doped TiO_2, Photocatalyst, co-precipitation method
DOI 10.14456/cast.1477.4

1. Introduction

Nowadays, the existence of organic pollutant in waste water is a worldwide topic for researchers and global environmental safety community [1]. Therefore, a complete removal of this toxic and organic dye is mandatory. Photocatalysis treatment has received great attention for removal of these organic toxic substances in aqueous phase.

Titanium dioxide (TiO_2) with anatase phase has been widely reported as the most favorable photocatalyst owing to its outstanding photocatalytic properties, together with an advantage in high photo-efficiency, strong oxidizing power, non-toxicity and low-cost [2-3]. However, pure TiO_2 photocatalyst has a large energy band gap of 3.2 eV, requiring ultraviolet (UV) light source for excitation, along with relatively high recombination rate of electron and hole pair. Thus, the photocatalytic performance of TiO_2 is expected to be inefficient under visible light or solar light irradiation, even with a lower rate of recombination rate. Many studies have been conducted for enhancing photocatalytic performance of TiO_2 by doping with suitable transition metal ions. Transition metal ion dopant can provide new energy levels within a band gap of the semiconductor

*Corresponding author: Tel.: +66 83-874-4045
E-mail: chakkaphan_w@rmutt.ac.th

that would result in lowering the excitation energy for an electron transfer from these levels to conduction band compared with pure TiO_2 catalyst [4]. Numerous types of transition metal ions have been studied as potential dopants, including chromium, manganese, iron, cobalt, nickel, copper and zinc [5-15]. It has been reported that incorporation of selective transition ions into TiO_2 could effectively enhance visible light response and photocatalytic efficiency. Devi *et al*. [16] studied the effect of Mn^{2+}, Ni^{2+} and Zn^{2+} in TiO_2 and their photocatalytic activities on aniline blue under ultraviolet and visible light irradiation. They suggested that Mn dopant could promote the mixing phase of anatase and rutile which showed the enhancement in photocatalytic activity under visible light irradiation. The different dopants of W, V, Ce, Zr, Fe and Cu were also utilized to adjust optical and photocatalytic properties of TiO_2 synthesized by a solution combustion method [17]. The synthesis of Co- and Mn-doped TiO_2 nanoparticles by hydrothermal method was reported for methylene blue dye decomposition under ultraviolet irradiation. Among these transition metal ion dopants, Co^{2+} ions have received much attention due to its suitable radius and energy level. The radius of Co^{2+} (0.078nm) closed to that of Ti^{4+} (0.068nm), indicating Co^{2+} ions easy to incorporate in TiO_2 lattice. Moreover, the cobalt doping has the positive effect through an introduction on catalyst such as an enhancement in invisible light absorption and increasing photo-excited electron-hole life time. Hence, in this study, the main objective was to develop TiO_2 nanoparticles by doping with Co at different contents by using a facile co-precipitation method. The performance of Co-doped TiO_2 to that of the bare TiO_2 for the degradation of rhodamine b (RhB) and methylene blue (MB) solution as a goal pollutant, general dyes used in the textile industry, was also compared.

2. Materials and Methods

Titanium isopropoxide *(*TTIP*)* and cobalt nitrate hexahydrate were used as a precursor of Ti and Co, respectively. Ammonia (NH_3) and absolute ethanol were used as a precipitation agent and solvent, respectively. TiO_2 doped with Co was synthesized by co-precipitation method, according to following steps. First, TTIP (14.2 ml) and cobalt nitrate (at 0.5, 1, 3 and 5 mol*%*) were weighed according to the required stoichiometric proportion and separately dissolved in absolute ethanol (100ml) under magnetic stirring for 20 min. Afterwards, both solutions were mixed together under vigorous stirring. Then, NH_3 solution was slowly loaded by drop-wise into the solution until pH 9 was achieved under stirring. The homogeneous solution was continuously stirred for 3 h. The solution was then aged for 24 h. The powders were washed by DI water to eliminate the impurity phase until the pH became 7. As synthesized powders were dried at 100°C for 24 h, the green powders were finally calcined at 500°C for 2 h.

The structural phase of Co-TiO_2 was studied by X-ray diffractometer (XRD); Rigaku Rint 2100 CMJ using CuK_α (λ=0.15406 nm). X-ray photoelectron spectroscopy (XPS); JEOL Ltd. model JPS-9010TRX, was used to study chemical composition of all samples. FESEM images were performed with Hitachi Model SU6600 scanning electron microscope. The optical properties were investigated by UV-vis diffused reflectance spectrometer (UV-Vis DRS)*:* Perkin Elmer model Lamda 750s. Typical dyes in the industry, RhB and MB were used as a model to evaluate the photocatalytic activity of prepared catalyst. The amount of catalyst added was 0.08 g in 100 ml of 0.01 mmol concentration of dyes solution. To guarantee the establishment of adsorption/desorption between catalyst and dye, the solution was stirred in the dark system for 20 min. The photocatalytic reaction was conducted at room temperature using Xenon lamp with 390 nm cutoff filter. The photocatalytic performance was determined by RhB and MB dyes degradation by checking the absorbance at λ_{max} = 554 and 663 nm, respectively, through a UV-Vis DRS.

3. Results and Discussion

The XRD diffraction patterns of Co-doped TiO_2 photocatalyst are shown in Figure 1. Their patterns clearly indicated that the main peak of pure TiO_2 and Co-doping sample located at $2\theta = 25.4$, 39.2, 48.0, 54.8 and 62.2 corresponding to the reflection from (101), (004), (200), (105) and (211). These observed patterns are nicely matched with the standard tetragonal anatase TiO_2. Furthermore, there is no characteristic peak corresponding to the secondary phases for oxides of dopants metal ions and rutile structure, indicating the good incorporation of Co ion dopant into TiO_2 matrix. Using full width at half maximum of predominant peak and Debye-Scherer formula, the crystalline size was estimated to be approximate value of 320, 239, 221, 215 and 202 nm for 0, 0.5 1, 3 and 5% dopant concentration, respectively. The reduction in crystalline size by increasing of dopant ions was observed in TiO_2 doped with transition metals like Fe and Ni. It is reported that the growth rate of TiO_2 nanocrystals on doping decreased due to the decreasing in the availability of growth sites of Ti ions as a result of the incorporation of dopant atoms. The occupation of specific growth sites of Ti atoms by dopant atoms inhibits further growth of TiO_2 nanoparticles.

X-ray photoelectron spectroscopy was used to determine insight of oxidation states for titanium, oxygen and cobalt metal cations in the samples and to ensure the chemical composition at surface layer of samples. The XPS survey scan (0-1300 eV) of 5 mol% Co-TiO_2 nanoparticles is displayed in Figure 2(a). The rough scanning spectra of doped sample reveal the existence of dopant ion, with main peaks from Co, O and Ti, confirming the chemical composition of major elements of Co-doped TiO_2 samples. For the identification of titanium oxide phase, it is noticed that that the splitting of Ti $2p_{3/2}$ and $2p_{1/2}$ binding energy located at 458.6 and 464.3 eV, respectively, is observable as seen in Figure 2(b). The separation of splitting binding energy is 5.7 eV, demonstrating a normal state of Ti with 4+ of oxidation state, which is attributed to the spin-orbit splitting of $Ti2p_{3/2}$ and $2p_{1/2}$ for Ti^{4+} in TiO_2 [12]. The binding energy of O1s is shown in Figure 2(c). The binding energy of samples could be deconvoluted into two constituents, synonymous to oxygen containing chemical bonds of water molecule (H-O-H) at 531.4 eV and hydroxyl (Co-O-H) at 530.1 eV [18]. Compared with bare-TiO_2 [12], the XPS peak position of $Ti2p_{3/2}$ and $Ti2p_{1/2}$ and O1s is at 458.3, 463.8 and 429.9 eV, respectively. It can be seen in current work that the slight shift of peak position after loading Co atoms was obtained. These results confirm the slight changing in TiO_2 structure. The XPS core level spectra of Co in the TiO_2 matrix are illustrated in Figure 2(d). The result demonstrates the binding energy values of $Co2p_{3/2}$ and $2p_{1/2}$ positioned at 781.1 and 796.9 eV, indicating that the Co elements could be in 2+ state [18].

Figure 3 shows the FESEM image and particle size distributions from several FESEM photographs of pure TiO_2 and Co-doped TiO_2 samples. As seen in micrographs, the powdered particle of pure TiO_2 consists of clusters of nanosized spherical primary particles, with average particle size around 330 nm. Meanwhile, the samples doped with different transition metal ions exhibit slightly smaller particle size at higher percentage of dopant and more agglomeration occurs with increasing doping content. The broaden peak in the particle size distribution increased with increasing of Co- content was observed. The average particle size of doped samples slightly decreases with increasing doping concentration, as a value of 240 - 210 nm. A slight decrease in the particle size and more agglomeration after loading higher Co ions could be due to the presence of an element in the TiO_2 compound. This presence causes a strain on the lattice and thus decrease the

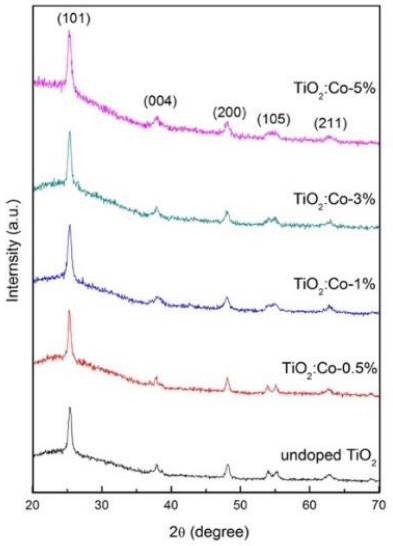

Figure 1. XRD patterns of Co-TiO_2 nanoparticles with various Co concentrations

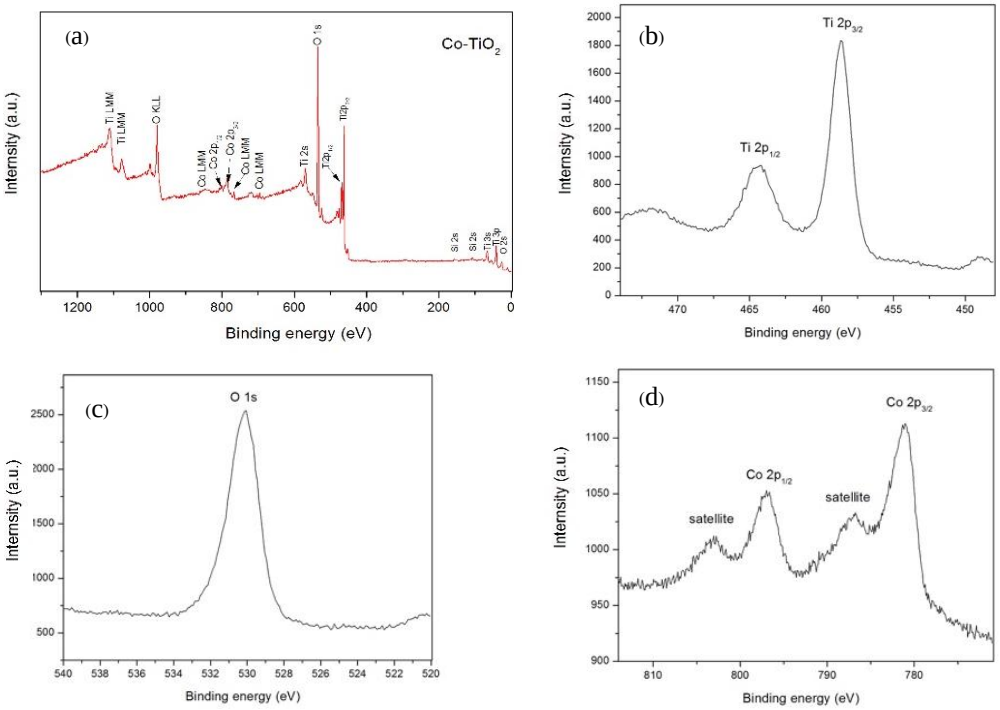

Figure 2. XPS spectrum of Co-TiO_2 with (a) Survey spectrum (b) core level spectrum of Ti, (c) core level spectrum of O and (d) core level spectrum of Co

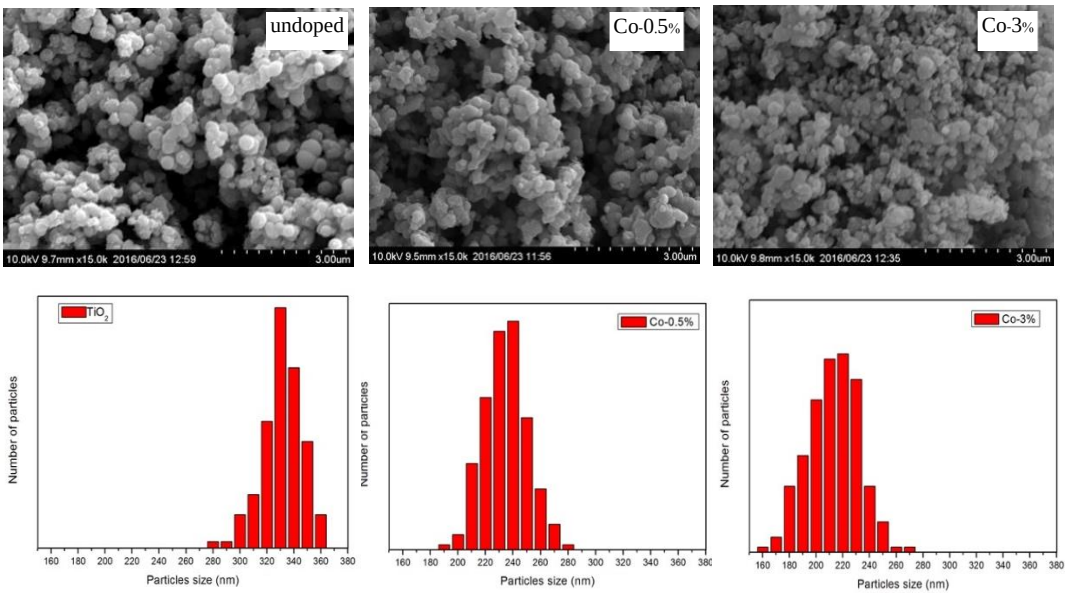

Figure 3. FESEM images and particle size distributions of undoped and Co-TiO_2 nanoparticles

lattice constant. By the smaller particles size, higher relative surface area and larger relative number of surface atoms were observed in the particles. Such surface atoms exhibit unsaturated coordination and each atom has vacant coordination sites. Thus, more bonds need to be formed to each surface atom. This causes an agglomeration in the prepared samples. The FESEM investigation suggests that the primary particle size could be responsible for the specific surface area of the powder. The specific surfaces of all samples were measured by BET technique. The undoped sample shows BET surface area of 48 m^2/g. Co-doped TiO_2 samples show their BET surface areas are in a range of 53, 56, 58 and 54 m^2/g for 0.5, 1, 3 and 5% of Co-content, respectively. Moreover, the doped samples represent the higher surface area when compared with undoped samples. Co-TiO_2 exhibited higher BET surface area that could result to the enhancement of photocatalytic behavior of the doped samples.

The UV-Vis DRS was used to determine the optical properties of the samples and corresponding spectra in the range of 250-700 nm for P-25 (for comparison), undoped and Co-TiO_2 samples and the results are exhibited in Figure 4. The reflectance spectra of P-25 and undoped sample display strong visible light reflection (>400nm). Meanwhile, the doped samples exhibit lower reflection in visible region; reflection spectra decrease with increasing doping concentration. From these results, it could be deduced that the addition Co-ion in the TiO_2 nanostructure can result in the amelioration in visible absorption. Moreover, the presence of Co-ion dopant may introduce the defect state located between the band gap that may allow TiO_2 to absorb light with lower energy than band gap energy. The incorporation of transition metal provides *d* orbitals below the conduction band that enables the ease of electron transfer from the valence band [9]. Typically, the band gap energy of the sample could be estimated using following equation: $(\alpha hv) = A(hv - E_g)^{1/2}$; where hv is the photon energy, α is the absorption coefficient which can be obtained from the reflectance spectra according to the Kubelka-Munk theory and A is a constant related to type of material. It is clearly noticed that the transition metal ions doped into TiO_2 significantly induce a prominent shift of band edge. The band gap value of Co-doped sample greatly decreases, with a value of 3.21, 3.05, 3.00, 2.75 and 2.95 eV as the doping content increases from 0, 0.5, 1, 3 and 5% of Co-content,

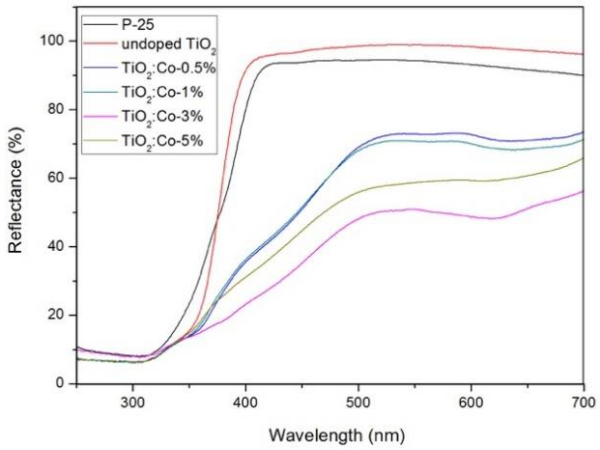

Figure 4. UV-Vis diffuse reflectance spectra of Co-TiO_2 samples with various Co-contents

respectively. It can be seen that the E_g of present work was narrower than the results reported in previous literature, for example E_g = 2.98, 2.97, 3.08 eV of Co-doped TiO_2 was claimed by Pirbazari *et al.* [19], Lee *et al.* [20] and Jiang *et al.* [21], respectively.

RhB and MB are representative of organic dyes in the textile effluents as seen in the functional groups in Figure 5 (a). These two organic compounds are often considered as a model contaminant in the photocatalytic decomposition in the waste water. Figures 5 (b) and (c) exhibit the photodegradation of RhB and MB in the presence of commercial sample P-25, undoped and Co-doped TiO_2 samples under visible light irradiation. It can be seen that the undoped samples show RhB degradation activity of ~ 19% in 270 min. In case of doped samples, the highest RhB photodecomposition was found in the 3% of Co-content with 82% of degradation. For the MB, the maximum decolorization of ~ 88% was found in the 3% of Co-content. Under the photocatalytic process, the photodecomposition mechanism can be described that the radicals in the solution attack principally at aromatic chromophore ring, leading to the degradation of RhB and MB structure. It could be deduced that the photocatalytic behavior of the samples highly depends on the dopant concentration. At small doping content, transition metal incorporated into TiO_2 may increase the lifetime of charge carrier resulting in the increasing photocatalytic performance. When the doping content exceeds the certain value, the number of crystal defects could be generated and may act as recombination centers resulting in the decrease of photocatalytic activity. Generally, the photocatalytic activity depends on several parameters such as phase structure, surface area and optical properties and so on. In this present work, the doping ions could induce insignificant change in the crystal structure. This may be attributed to the effect on the impurity levels in the energy band gap of TiO_2 host catalyst. For the other possible reason, the addition of transition metal ion might produce new trapping site which affects the life-time of charge carriers [13]. Moreover, it can be seen that the photocatalytic rate constant of degradation for MB is higher than that of RhB as shown in Figures 5 (d) and (e). This may be attributed to the difference in the chemical structure and nature functional groups of dyes, resulting in the different absorption characteristics and difference in susceptibility to photodegradation. The chemical structure of RhB dye is more complex, making it

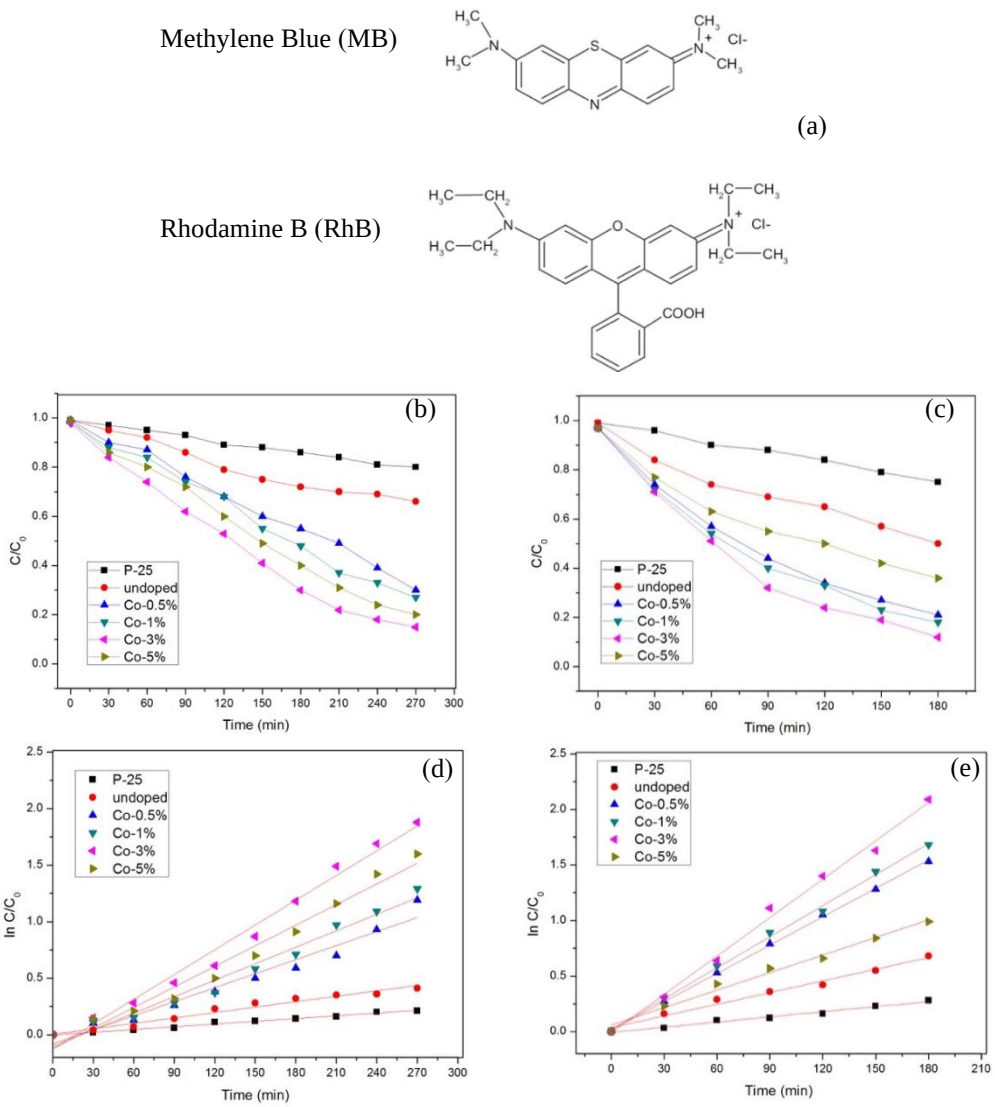

Figure 5. Functional group of MB and RhB dyes (a) with their photodegradation: RhB (b), MB (c) and their rate constant of photodegradation: RhB (d), MB (e) in presence of P-25, undoped and Co-TiO_2 nanoparticles under visible light irradiation and photodegradation

less photodegradable. By comparing to the previous work for transition metal ions doping, it is observed that the results of this work are slightly higher than the prior reported. For example, Pirbazari *et al*. [19] have claimed that the Co/TiO_2 prepared by sol-gel method exhibits 100% and 60% of MB dye degradation within 210 min under UV and visible light irradiation, respectively.

4. Conclusions

The Co-doped TiO_2 catalysts with doping content of 0.5-5 mol% were synthesized via simple co-precipitation method combined with annealing process at 500°C for 2 h. The structural phases of all samples belong to the anatase TiO_2 without impurity phase of oxide compounds. The XPS results exhibit the existence of Co in the host samples, confirming the oxidation state of 4+ and 2+ for Ti and Co, respectively. The Co dopant introduced into TiO_2 catalyst leads to the increase of surface area and visible light optical absorption response. The band gap energies of all samples decrease with increasing doping Co content. The amount of dopant directly affected the photocatalytic efficiency of photocatalyst. Both RhB and MB dyes were highly degraded by TiO_2 doped with 3% of Co. The difference of dopant concentration has strong influence on phase structure, morphology, optical properties and also photocatalytic activity of TiO_2 sample.

5. Acknowledgements

The authors are grateful to Division of Physics, Faculty of Science and Technology, Ragamangala University of Technology Thanyaburi (RMUTT) and Smart Materials Research Unit (SMRU) for supporting the facilities.

References

[1] Ahmed, S., Rasul, M.G., Brown, R. and Hashib, M.A., 2011. Influence of parameters on the heterogeneous photocatalytic degradation of pesticides and phenolic contaminations and waste water. *Journal of Environmental Management*, 92, 311-330.

[2] Hoffmann, M.R., Martin, S.T., Choi, W. and Bahnemann, D.W., 1995. Environmental Application of semiconductor photocatalysis. *Chemical Reviews,* 95, 69-96.

[3] Litter, M.I., 1999. Heterogeneous photocatalysis: Transition metal ion in photocatalytic system. *Applied Catalysis B: Environmental*, 23, 89-114.

[4] Choi, J., Park H. and Hoffmann, M.R., 2010. Effects of single metal-doping on visible light photoreactivity of TiO_2. *Journal of Physical Chemistry C*, 114, 783-792.

[5] Ananpattarachai, J. and Kajitvichyanukul, P., 2016. Enhancement of chromium removal efficiency on adsorption and photocatalytic reduction using a bio-catalyst, titania-impregnated chitosan/xylan hybrid film. *Journal of Cleaner Production*, 130, 126-136.

[6] Chauhan, R**.**, Kumar, A**.** and Chaudhary, R.P., 2012. Structural and photocatalytic studies of Mn doped TiO_2 nanoparticles**.** *Spectrochemica Acta Part A: Molecular and Biomolecular Spectroscopy*, 98, 256-264**.**

[7] Moradi, H., Eshaghi, A., Hosseini, S.R. and Ghani, K., 2016. Fabrication of Fe-doped TiO_2 nanoparticles and investigation of photocatalytic decolorization of reactive red 198 under visible light irradiation. *Ultrasonic Sonochemistry*, 32, 314-319.

[8] Junlabut, P., Wattanawikkam, C., Phoohinkong, W., Mekprasart, W. and Pecharapa, W., 2016. Effect of cobalt on structural and optical properties of co-precipitated TiO_2 nanopowders. *Key Engineering Materials*. 675/676, 97-100.

[9] Yadav, H.M., Otari, S.V., Bohara, R.A., Mali, S.S., Pawar, S.H. and Delekar, S.D., 2014. Synthesis and visible light photocatalytic antibacterial activity of nickel-doped TiO_2

nanoparticles against Gram-positive and Gram-negative bacteria. *Journal of Photochemistry and Photobiology A: Chemistry*, 294, 130-136.

[10] Wattanawikkam, C., Pecharapa, W. and Ishihara, K. N., 2017. X-ray absorption spectroscopy analysis and magnetic properties of M-doped TiO_2 nanoparticles (M=Co, Mn, Ni and Zn) prepared by co-precipitation method. *Ceramics International*, 43, S397-S402.

[11] Singla, P., Sharma, M., Pandey, O.P. and Singh, K., 2014. Photocatalytic degradation of azo dyes using Zn-doped and undoped TiO_2 nanoparticles. *Applied Physics*, 116, 371-389.

[12] Reddy, S., Boningari, T. and Suidan, M., 2014. Visible-light-induced photodegradation of gas phase acetonitrile using aerosol-made transition metal ion (V, Cr, Fe, Co, Mn, Mo, Ni, Cu, Y, Ce and Zr) doped TiO_2. *Applied Catalysis B: Environmental*, 114, 333-342.

[13] Tripathi, A.K., Mathpal, M.C., Kumer, P., Singh, M.K., Soler, M.A.G. and Garwal, A.A, 2015. Structural, optical and photoconductivity of Sn and Mn doped TiO_2 nanoparticles. *Journal of Alloys and Compounds*, 622, 37-47.

[14] Park, J.Y., Choi, K.I., Lee, J.H., Hwang, C.H., Choi, D.Y. and Lee, J.W., 2013. Fabrication and characterization of metal-doped TiO_2 nanofibers for photocatalytic reactions. *Materials Letters*, 97, 64-66.

[15] Jing, L., Xin, B., Yuan, F., Xue, L., Wang, B. and Fu, H., 2006. Effect of surface oxygen vacancy on photochemical and photochemical processes of Zn-doped TiO_2 nanoparticles and their relationships. *Journal of Physical Chemistry B*, 110, 17860-17865.

[16] Devi, L G., Kottam, N., Murthy, B. N. and Kumar, S. G., 2010. Enhanced photocatalytic activity of transition metal ions Mn^{2+}, Ni^{2+} and Zn^{2+} doped polycrystalline titania for the degradation of Aniline Blue under UV/solar light. *Journal of Molecular Catalysis A: Chemical*, 328, 44-52.

[17] Nagaveni, K. K., Hegde, M.S. and Madras, G., 2004. Structural and photocatalytic activity of $Ti_{1-x}MxO_{2+/-delta}$ (M=W, V, Ce, Zr, Fe, and Cu) synthesized by solution combustion method. *The Journal of Physical Chemistry B*, 108, 20204-20212.

[18] Tan, B. J., Klabunde, K.J., and Peter, M. A., 1991. XPS studies of solvated metal atom dispersed catalysts. evidence for layered cobalt-manganese particles on alumina and silica. *Journal of the American Chemical Society*, 133, 855-581.

[19] Pirbazari, A.E., Monazzam, P.P. and Kisomi, B.F., 2017. Co/TiO_2 nanoparticles: preparation, characterization and its application for photocatalytic degradation of methylene blue. *Desalination and Water Treatment*, 63, 283-292.

[20] Lee, H., Park, Y.K., Kim, S.J., Kim, B.H. and Jung, S.C., 2015. Titanium dioxide modification with cobalt oxide nanoparticles for photocatalysis. *Journal of Industrial and Engineering Chemistry*, 32, 259 -263.

[21] Jiang, P., Xiang, W., Kuang, J., Liu, W. and Cao, W., 2015. Effect of cobalt doping on the electronic, optical and photocatalytic properties of TiO_2, *Solid State Sciences*, 46, 27-32.